

Mutational fingerprints of aging

Martijn E. T. Dollé*, Wendy K. Snyder, David B. Dunson¹ and Jan Vijg

Sam and Ann Barshop Center for Longevity and Aging Studies, University of Texas Health Science Center, 15355 Lambda Drive, STCBM 2.200, San Antonio, TX 78245, USA and ¹Biostatistics Branch, National Institute of Environmental Health Sciences, Research Triangle Park, NC 27709, USA

Received August 27, 2001; Revised November 7, 2001; Accepted November 15, 2001

ABSTRACT

Using a *lacZ* plasmid transgenic mouse model, spectra of spontaneous point mutations were determined in brain, heart, liver, spleen and small intestine in young and old mice. While similar at a young age, the mutation spectra among these organs were significantly different in old age. In brain and heart G:C→A:T transitions at CpG sites were the predominant mutation, suggesting that oxidative damage is not a major mutagenic event in these tissues. Other base changes, especially those affecting A:T base pairs, positively correlated with increasing proliferative activity of the different tissues. A relatively high percentage of base changes at A:T base pairs and compound mutants were found in both spleen and spontaneous lymphoma, suggesting a possible role of the hypermutation process in splenocytes in carcinogenesis. The similar mutant spectra observed at a young age may reflect a common mutation mechanism for all tissues that could be driven by the rapid cell division that takes place during development. However, the spectra of the young tissues did not resemble that of the most proliferative aged tissue, implying that replicative history *per se* is not the underlying causal factor of age-related organ-specific differences in mutation spectra. Rather, differences in organ function, possibly in association with replicative history, may explain the divergence in mutation spectra during aging.

INTRODUCTION

Somatic mutations are thought to play a major causal role in cancer and, possibly, aging (1,2). To monitor tissue-specific patterns of somatic mutation accumulation during aging, a plasmid transgenic mouse model sensitive to a broad range of mutational events has been developed (3). These mice harbor chromosomally integrated plasmids that can be efficiently recovered from genomic DNA and transferred into a suitable *Escherichia coli* host for mutant selection, quantitation and characterization. The advantages of this system include an extensive choice of tissue types suitable for mutation examination and the absence of any selection pressure *in vivo* of a mutation in the neutral reporter. On the other hand, mutagenic events

coupled to transcription might be under-represented or not detected at all in the silent reporter gene.

Using the plasmid transgenic mouse model, we have previously reported organ-specific differences in mutation accumulation with age (4,5). Further characterization of the mutational spectra as they unfold in old age could provide molecular fingerprints to obtain an insight into the possible sources of molecular damage, which has been implicated as the ultimate cause of aging and its associated diseases (6,7). Here we specifically compare the point mutational spectra in five organs, with different proliferative histories, in young and old mice and in lymphomas, the most frequent neoplastic lesion in old age in these mice. The results indicate that the mutation spectra in the different organs diverge during the aging process. It is suggested that the organ-specific mutation spectra emerging in old age reflect a combination of the proliferative history and unique function of each organ.

MATERIALS AND METHODS

Plasmid rescue

Aging cohorts of male C57Bl/6 pUR288-*lacZ* mice of line 60 were maintained in the animal facilities of the Beth Israel Deaconess Medical Center (Boston, MA) as described previously (4). The animals were killed by decapitation following asphyxiation with CO₂. Organs and tissues were removed, rinsed in PBS, placed in 1.5 ml microcentrifuge tubes and frozen on dry ice. Any macroscopic lesions observed during tissue collection were excised and stored separately. The tissues were maintained at -80°C until used. DNA was extracted by routine phenol/chloroform extraction. Complete protocols for plasmid rescue and mutant frequency determinations with this model are given elsewhere (8). Briefly, between 10 and 20 µg genomic DNA was digested with *Hind*III for 1 h in the presence of magnetic beads (Dynal) pre-coated with *lacI-lacZ* fusion protein. The beads were washed three times to remove the unbound mouse genomic DNA. Plasmids were subsequently eluted from the beads with IPTG. After circularization of the plasmids with T4 DNA ligase they were ethanol precipitated and used to electrotransform *E. coli* C (Δ *lacZ*, *galE*⁻) cells. One-thousandth of the transformed cells were plated on a titer plate (with X-gal) and the remainder on a selective plate (with *p-gal*). The plates were incubated for 15 h at 37°C. Mutant frequencies were determined as the number of colonies on the selective plates versus the number of colonies on the titer plate (times the dilution factor of 1000).

*To whom correspondence should be addressed. Tel: +1 210 562 5027; Fax: +1 210 562 5028; Email: dollé@uthscsa.edu

Mock-recovery

To check for a possible *E. coli* contribution to the spontaneous mutation spectra as observed in the *lacZ* plasmids obtained from the mouse, the same plasmids were grown in *E. coli*. For these experiments, *E. coli* C cells harboring the wild-type pUR288 plasmid were obtained in the form of a dark blue staining colony on a titer plate from a regular mutant frequency determination. These cells were grown in 3 ml of LB medium containing 75 µg/ml ampicillin and 25 µg/ml kanamycin for 8 h at 37°C at 225 r.p.m. Cells were harvested by centrifugation for 10 min at 1000 g. DNA was extracted by routine phenol/chloroform extraction. The plasmid preparations were mixed with non-transgenic liver DNA, after which mutant plasmids were recovered as described above for genomic DNA isolation.

Mutant classification

Mutant colonies were taken from the selective plates and grown overnight in 3 ml of LB medium. Then, 1 µl was directly plated onto X-gal to screen for galactose-insensitive host cells (9). The remainder of the cell culture was used for plasmid mini preparation (Wizard 9600; Promega). The purified plasmids were digested with *Pst*I and *Ava*I and size separated on 1% agarose gels. Mutant plasmids with restriction patterns resembling and deviating from the wild-type restriction pattern were classified as 'no-change' and 'size-change' mutants, respectively.

Sequencing

Sequencing reactions were performed with the CEQ dye terminator cycle sequencing kit (Beckman, Fullerton, CA), according to the manufacturer's standard protocol, and analyzed with a CEQ 2000 DNA analysis system (Beckman). The primers used were as described earlier (9).

RESULTS AND DISCUSSION

Mutant *lacZ* plasmids were recovered from brain, heart, liver, spleen and small intestine of young (3–4 months) and old (30–33 months) pUR288 C57Bl/6 mice and subdivided, based on size, into no-change and size-change mutants. From the no-change mutants, which were presumed to be point mutations, 20–22 were randomly selected per age/organ group from three to four animals and completely sequenced (Table 1). The point mutational spectra, limited to base changes and single base deletions, of the five organs in the two age groups are expressed as mutant frequencies in Figure 1. Statistical analyses of the mutational frequencies and spectra were conducted using a Bayesian approach (10). In testing for differences in the mutational spectra between groups, the mean square error was used as the measure of discrepancy.

The total and categorized point mutation frequencies were higher on average for the older mice (*a posteriori* P value < 0.01). An increase in the frequency of all point mutations was observed in the heart (P < 0.01), liver (P < 0.01), spleen (P = 0.01) and small intestine (P < 0.01), but not in the brain (P = 0.41). The magnitude of the difference between young and old mice was higher in the small intestine than in the other organs (P = 0.05). There were also clear differences between age groups in the proportions of mutations falling into the different subclasses (P < 0.01). This difference was evident in the brain (P < 0.01),

spleen (P = 0.03) and small intestine (P = 0.03), but not in the heart (P = 0.13) or liver (P = 0.88). In addition to these effects, the old mice exhibited clear differences between organs in both the mutation frequencies (P < 0.01) and subclass proportions (P < 0.01). However, such differences were not apparent among the younger mice (P = 0.09 and P = 0.81, respectively).

The point mutational spectra in the five organs, which are similar at a young age, diverge in a way that, at least in part, seems to reflect their proliferative history over the lifespan of the mouse. The organs in Figure 1 have been arranged from left to right by increasing proliferative activity. Studies comparing DNA-incorporated radioactivity per organ after administration of [³H]thymidine clearly set the small intestine apart from the other four organs in terms of proliferative activity (11,12). Spleen is the second most proliferative organ among the five organs studied. Both Kupffer and parenchymal cells contributed to some remaining proliferative activity in the liver (11). Based on the cardiomyocytes, the heart is virtually a post-mitotic organ, but some proliferative activity, possibly due to other cell types, has been found (12). Brain appears to be virtually devoid of proliferative activity (11,12). From our present studies it appears that G:C→A:T transitions at CpG sites correlate strongly with a lack of proliferative activity over a lifetime (Fig. 1). Other base changes than G:C→A:T transitions emerge with increasing frequency from brain to small intestine, the latter organ being dramatically different, with relatively high frequencies of G:C→A:T at non-CpG sites, G:C→T:A, G:C→G:T and base changes at A:T base pairs. In general, while G:C→A:T transitions at CpG sites are predominantly found in post-mitotic organs, changes at A:T base pairs correlate positively with proliferative activity (Fig. 1).

The increase in G:C→A:T transitions at CpG sites in the brain and heart indicates that the predominant mutational mechanism in post-mitotic tissue during aging is spontaneous deamination of 5-methylcytosine. As proposed by MacPhee (13), mismatch repair would have a 50% chance of reverting a C:T mismatch to the original sequence and a 50% chance of creating a stable G:C→A:T transition in the absence of proper strand recognition signals. However, most spontaneous deaminations of 5-methylcytosine are repaired correctly, for instance by specific glycosylases (14).

Oxidative stress has been suggested to play an important role in aging, damaging DNA and other macromolecules alike (15). Because our data indicate that age-related mutation accumulation in the brain and heart is mainly due to spontaneous deamination of 5-methylcytosine, oxidative damage does not seem to be a major mutagenic event in these tissues. In this respect, it is conceivable that the relatively high rate of oxidative metabolism in brain and heart mainly causes mutations in the mitochondrial genome (16), while oxidative damage to the nuclear genome of these post-mitotic tissues might be repaired without a mutagenic consequence.

A question of major importance is the source of the mutations in the more proliferative organs, most notably the small intestine, which are likely to be caused by misreplication at damaged sites. In this respect, at least two possibilities come to mind. First, oxidative damage might play a role, since predominantly G:C base pairs were affected (Fig. 1). G or C bases have been identified as the main target for oxidative damage *in vitro* (17). Second, replication errors may also arise as a consequence of DNA lesions induced by environmental mutagens,

Table 1. Sequenced *lacZ* no-change mutations recovered from brain, liver, spleen and lymphoma of 3.5- and 32-month-old mice

Brain				Liver				Spleen				Lymphoma			
Base position ^a	pUR288 sequence (5'→3')	Alteration	Frequency ^b	Base position ^a	pUR288 sequence (5'→3')	Alteration	Frequency ^b	Base position ^a	pUR288 sequence (5'→3')	Alteration	Frequency ^b	Base position ^a	pUR288 sequence (5'→3')	Alteration	Frequency ^b
----- 3.5-month -----															
274	ACAACC C TGGCGT	delC		392	CGAATG G CGCTTT	G→A		357	GATCGC C CTTCCC	C→G					
487	CAAAC T GCAGAT	G→A		487	CAAAC T GCAGAT	G→A		378	CGCAGC C TGAATG	C→A					
981	TACCTA C GGGTAA	delC		647	TATTTT T GATGGC	delT		392	CGAATG G CGCTTT	G→A					
1411	CGCTGT G GIACAC	G→A		748	CATTTT T ACGCGC	delT		429	GTGCCG G AAAGCT	G→T					
1595	GCTGGG G AATGAA	delG		1876	AATACT G GCAGCG	G→A		827	TATGTG G CCGATG	G→A					
1673	GGTGCA G TATGAA	G→C		2283	CAGCCG G AGAGCG	G→T		1145	TCTCTA T CGTGGC	T→G					
2877	AACTGC C AGCTGG	C→T		2562	CTGGCC G ATCAGT	delG		1186	CGCTGA T TGAAGC	T→C					
1746	GAAGAC C AGCCCT	C→T						1200	GAAGCC T GCGATG	T→C					
				403	TTGCCT G GTTTCC	G→A		1290	CGTCAC G AGCATC	G→A ^c					
879	ACTACA C AAATCA	C→T		1014	GAAACG C AGGTGC	C→T		1396	ATTATC C GAACCA	C→T ^c					
1283	CGTTAA C CGTCAC	C→A		1160	GGTTGA A CTGCAC	delA		1726	CGATGT A CGCGCG	A→G					
1727	GATGTA C GCGCGC	C→A		1387	GCTGTT C GCATTA	C→T ^c	2	2540	TAAAAA A CAACTG	delA					
1827	CTTTGC G AATACG	G→C	3	2100	TTTTTC C AGTTCC	C→T		2613	GAAGCG A CCCCA	delA					
2574	TTCACC C GTGCAC	C→T ^c		2540	TAAAAA A CAACTG	delA									
419	ACCAGA A GCGGTG	delA		537	TATCCC A TTACGG	delA		844	GCATTT T CCGTGA	delT					
694	GCTGGG T CGGTAA	delT		1673	GGTGCA G TATGAA	G→C		1396	ATTATC C GAACCA	C→T ^c					
984	CTACGG G TAACAG	delG		1396	ATTATC C GAACCA	C→T ^c		2277	CTACCG C AGCCGG	C→T					
1859	TCTTGG C GGTTTC	delC		1542	GTAACG C GAATGG	C→T ^c		2487	CGTTGG C AATTTA	C→T					
2179	TGCACT G GATGGT	G→A		1687	GCGCGG G AGCCGA	delG		708	GGCCAG G ACAGTC	G→C					
2341	CCGCAT G GTCAGA	G→A		2640	TGGGTC G AACGCT	G→T		790	TGCCTT G GAGTGA	G→A					
2939	CTATCC C GACCGC	delC		2859	CCGGCC G GGATTG	C→T ^c		838	TGAGCG G CATTTT	G→A					
				3117	CAGCAA ctga TGGAAA	4bp del		1369	ACAAC T taae GCCGTG	5bp del					
								1673	GGTGCA G TATGAA	G→C					
								1673	GGTGCA G TATGAA	G→C					
								1784	CAAAAA A TGGCTT	delA					
								2369	CGCCTG G CAGCAG	G→A					
----- 32-month -----															
837	ATGAGC G GCATTT	G→A ^c		403	TTGCCT G GTTTCC	G→A		633	GGCCAG A CGCGAA	A→C		1410	CCGCTG T GGTACA	T→C	2
1272	CTGATT C GAGGCG	C→T ^c		637	AGACGC G AATTAT	delG		2538	GATAAA A AACAAC	A→T		3054	TTGAAT T ATGGCC	T→G	5
1290	CGTCAC G AGCATC	G→A ^c		1387	GCTGTT C GCATTA	C→T ^c		1525	CGCGCA T GAGCGA	T→G		3068	ACAACA G TGGGCG	G→C	
1290	CGTCAC G AGCATC	G→A ^c		2487	CGTTGG C AATTTA	C→T		1792	GGCTTT C GCTACC	C→A					
1290	CGTCAC G AGCATC	G→A ^c		2792	CCGGAT T GATGTT	T→TT		1827	CTTTGG G AATACG	G→A ^c		250	TCGTTT T ACAACG	T→A	
								2693	CGAGTG C ACGCA	C→A		1230	CGGATT G AAAATG	G→T	
543	ATTACG G TCAATC	delG		1272	CTGATT C GAGGCG	C→T ^c						1438	ACGGCC T GTATGT	T→C	
1272	CTGATT C GAGGCG	C→T ^c	2	1771	CGAAAT G GTCCAT	G→A		1594	CGCTGG G GAATGA	G→T		1634	GCTGTA T CGCTGG	T→C	3
1290	CGTCAC G AGCATC	G→A ^c		1947	CTGATT A AATATG	A→T		1737	CGCGTG gatg AAGACC	4bp del		2991	TCAGAC A TGTATA	A→G	
1373	CTTTAA C GCCGTG	delC		2667	CATTAC C AGGCGC	C→T		2241	GCTCCA C AAGGTA	C→T		3022	GCGAAA A CGGTCT	A→T	
				2913	TGGCTC G GATTAG	G→A ^c		2913	TGGCTC G GATTAG	G→A ^c		1934	GGTGGG T CAGTCG	delT	
1396	ATTATC C GAACCA	C→T ^c						3175	TGAATA T CGACGG	T→A		2342	CGCATG G TCAGAA	G→A	
1465	ATATTG A AACCCA	A→C		1027	CCAGCG G CACCGC	delG									
1585	TCATCT G GTCGCT	G→A		1272	CTGATT C GAGGCG	C→T ^c		837	ATGAGC G GCATTT	G→A ^c		651	TTTGAT G GCGTTA	C→G	2
1746	GAAGAC C AGCCCT	C→T		1673	GGTGCA G TATGAA	G→C		1128	AGCGCC G AAATCC	G→A ^c		1396	ATTATC C GAACCA	C→T ^c	3
2562	CTGCGC G ATCAGT	G→A ^c		1792	GGCTTT C GCTACC	C→A		1290	CGTCAC G AGCATC	G→A ^c		1827	CTTTGC G AATACG	G→A ^c	2
				2743	ACGCGT G GCAGCA	G→A		1839	GCCAC GC AGTGGG	GC→TA					
1290	CGTCAC G AGCATC	G→A ^c		2942	TCCCGA CC GCCTTA	CC→AT		2996	CATGTA T ACCCCG	T→G					
1290	CGTCAC G AGCATC	G→A ^c													
1784	CAAAAA A TGGCTT	delA		879	ACTACA C AAATCA	C→T		516	CCCATC T ACACCA	T→G					
1784	CAAAAA A TGGCTT	delA		1586	CATCTG G TCGCTG	G→A		609	GTTGAT G AAAGCT	G→T					
2905	GGTAA A CTGGCT	delA		1784	CAAAAA A TGGCTT	delA		748	CATTTT T ACGCGC	T→G					
				1982	GGCTTA C GCGGCT	C→A		825	GATATG T GCGGGA	T→C					
				2967	TTTGAC C GCTGGG	delC		2540	TAAAAA A CAACTG	delA					

Empty lines separate mutants obtained from individual mice. The cross-hatched areas indicate compound mutants; all other mutants contained single mutations. Sequence data on point mutations for heart and small intestine have been published elsewhere (5).

^aNucleotide numbering according to SYNPUR288V (GenBank accession no. L09147).

^bFrequency of recurrent mutations, i.e. identical mutants recovered from the same tissue sample. Other seemingly recurrent mutations in this table were unique, based on the presence of different polymorphic markers among the mutated plasmids. (These single nucleotide polymorphisms were shown to be present among the integrated wild-type plasmid copies of this transgenic mouse model; 26.)

^cG:C→A:T base change at a CpG site.

taken up with food by the small intestine or detoxified in the liver.

In old spleen a relatively high percentage of base changes was found to involve A:T base pairs (Fig. 1). This is in keeping with the observed point mutational spectra of both human and mouse lymphocytes at the *Hprt* locus (18,19). In this respect, it appears that *Hprt* mutation spectra in blood lymphocytes are not representative of other cell and tissue types. Interestingly, a high frequency of base changes at A:T was also found in the mutation spectrum of spontaneous lymphomas isolated from old mice (Fig. 2). Two of the fourteen unique lymphoma

mutants sequenced contained multiple mutations, i.e. 14%. In spleen, the main target organ for lymphomas in aging mice, the frequency of *lacZ* mutants containing two or more mutations was 10%, while averaging only 2% in the other four organs (Table 1). We interpret the high percentage of such compound mutants as evidence for a temporal burst of mutational activity at some point in the history of these tissues. As such, this finding is in keeping with the mutator phenotype postulated to underlie the initiation and progression of tumors (20). It is tempting to speculate that somatic hypermutation, a predominantly point mutational process improving the affinity of Ig

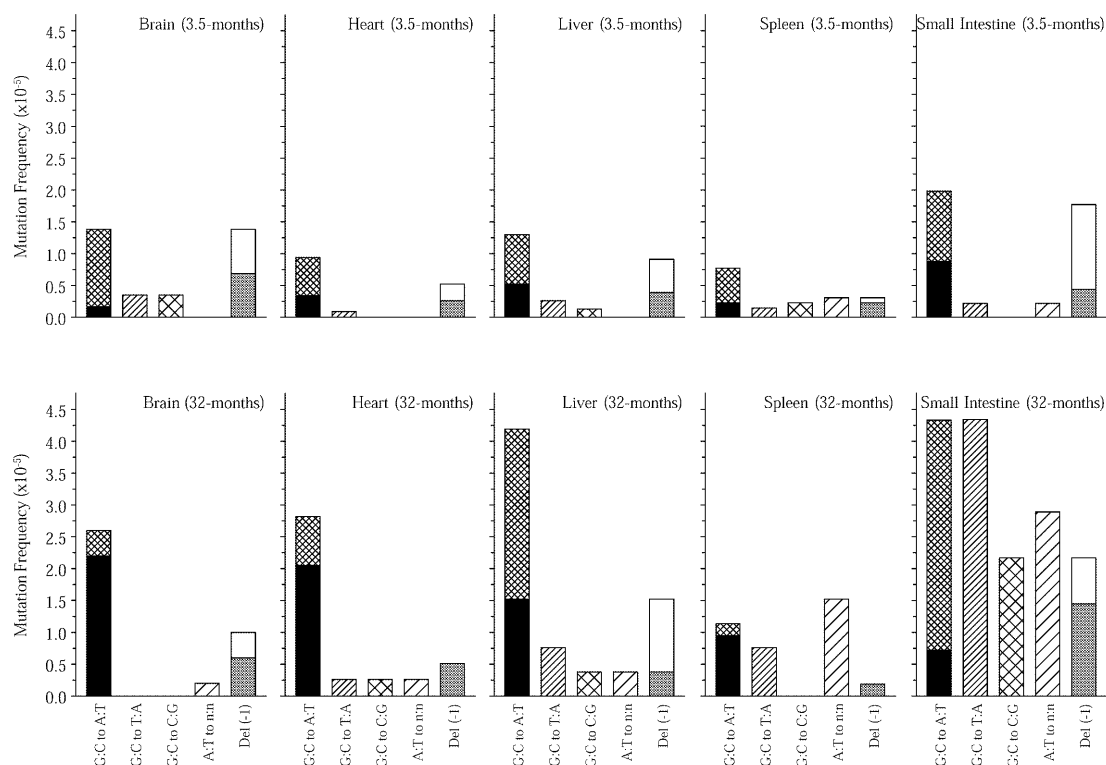


Figure 1. Point mutational spectra of the *lacZ* reporter gene in brain, heart, liver, spleen and small intestine from young (3.5 months) and old (32 months) mice. Bars represent the frequency of each type of point mutation as indicated. The black areas in the G:C→A:T bars indicate the fraction of such mutations that had occurred at CpG sites and the gray areas in the Del (-1) bars indicate the fraction of such mutations that had occurred at reiterated sites, i.e. a sequence of three or more of the same nucleotide. Corrections for recurrent mutations were made.

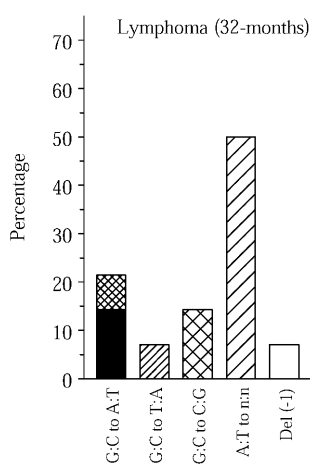


Figure 2. Point mutational spectra of the *lacZ* reporter gene in spontaneous lymphomas found in old mice. See legend to Figure 1 for an explanation of the bars. Mutational spectra are expressed as percentages to omit inaccuracies in correcting mutant frequencies for frequent recurrent mutations leading to a small number of unique plasmids analyzed for some lymphomas (Table 1).

molecules in germinal centers in lymph nodes and spleen, causes such compound mutants, which may increase cancer risk. Recently, somatic hypermutation has been associated with DNA polymerase η as an A:T mutator (21,22), which could explain the relatively large fraction of mutations found at A:T base pairs in old spleen and lymphoma (Figs 1 and 2).

While the observed mutation spectrum in the spleen could be causally related to the etiology of lymphomas, the same does

not apply to the small intestine. Indeed, while small intestine has the highest spontaneous mutation rate of all tissues tested (Fig. 1) (5), tumors in this tissue occur at very low frequencies (23). Possibly, other factors than somatic mutation rate alone play a role in determining susceptibility of an organ to tumor formation. In this respect, it should be noted that mice deficient for the mismatch repair genes *Mlh1* and *Pms2* show 18- and 13-fold increases in point mutations in the small intestine at a *lacI* transgene (24), respectively, which did not dramatically increase the frequency of small intestinal tumors (25).

At a young age the mutation spectra in brain, heart, liver, spleen and small intestine are remarkably similar (Fig. 1). To exclude the possibility that this similarity is due to a background level of mutations due to the rescue process, a point mutational spectrum from mock-recovered plasmids grown in *E.coli* was determined (Fig. 3). Although the mock-recovered spectrum resembled the spectra of the young mouse tissues (Figs 1 and 3), the mock-recovered point mutant frequency was only $\sim 0.6 \times 10^{-5}$, as compared with 2.8×10^{-5} on average in tissues from young animals. Furthermore, the mock-recovered mutant frequency is an overestimate due to the inability to obtain mutation-free starting material, i.e. wild-type plasmid preparations. Based on our previous results (26), many of the mutations occur during growth in *E.coli* prior to plasmid preparation and not during mock recovery. Indeed, when the sites of the base changes were taken into account, many of the mock-recovered mutants turned out to be unique, i.e. only 17% of the point mutations were found among 140 different point mutations recovered from the mouse. The young mouse tissues

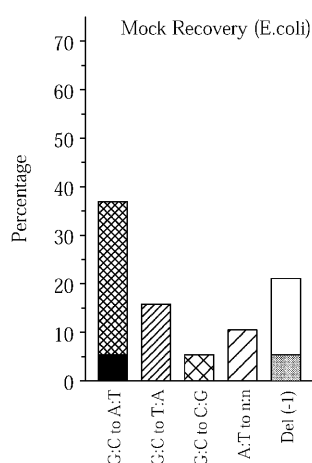


Figure 3. Point mutational spectra of mock-recovered plasmids grown in *E.coli* C. See legend to Figure 1 for an explanation of the bars. Mutational spectra are expressed as percentages, since thus far there is no evidence that they represent a real background, i.e. find their origin in the rescue process (see text).

Table 2. Number of identical point mutations found in the *lacZ* transgene of other mouse tissues

Source	Compared	Matching	Percentage
Young brain	20	5	25
Young heart	20	10	50
Young liver	20	11	55
Young spleen	23	8	35
Young small intestine	19	6	32
Average young mouse tissues			39
Mock-recovery (<i>E.coli</i>)	18	3	17

The mouse database comprised 140 unique point mutations.

shared on average 39% of their point mutations with this mouse mutation database (Table 2).

Hence, we believe that the mutation spectra in the young somatic tissues (Fig. 1) are genuinely similar, which suggests that, in contrast to aging, development is associated with a mutation mechanism common to all cells and tissues. In this respect, one would suspect that these early mutation spectra are associated with replication errors and, hence, resemble the spectra in actively proliferating tissue, such as spleen and small intestine, at a greater age. However, this is not the case, which suggests that replicative history *per se* is not the underlying causal factor of age-related organ-specific mutation spectra. Rather, differences in organ function, possibly in association with replicative history, may explain the divergence in mutation spectra during aging. Such *in vivo* mutational fingerprints are likely to provide clues as to the various sources of somatic damage thought to underlie age-related cellular degeneration and death under various environmental conditions.

ACKNOWLEDGEMENTS

This work was supported by grants 1PO1AG17242-01, AG13319-05 and 1RO1CA75653-03.

REFERENCES

- Vijg, J. (2000) Somatic mutations and aging: a re-evaluation. *Mutat. Res.*, **447**, 117–135.
- DePinho, R.A. (2000) The age of cancer. *Nature*, **408**, 248–254.
- Boerrigter, M.E.T.I., Dollé, M.E.T., Martus, H.-J., Gossen, J.A. and Vijg, J. (1995) Plasmid-based transgenic mouse model for studying *in vivo* mutations. *Nature*, **377**, 657–659.
- Dollé, M.E.T., Giese, H., Hopkins, C.L., Martus, H.-J., Hausdorff, J.M. and Vijg, J. (1997) Rapid accumulation of genome rearrangements in liver but not in brain of old mice. *Nature Genet.*, **17**, 431–434.
- Dollé, M.E.T., Snyder, W.K., Gossen, J.A., Lohman, P.H. and Vijg, J. (2000) Distinct spectra of somatic mutations accumulated with age in mouse heart and small intestine. *Proc. Natl Acad. Sci. USA*, **97**, 8403–8408.
- Kirkwood, T.B. and Austad, S.N. (2000) Why do we age? *Nature*, **408**, 233–238.
- Vijg, J. and Dollé, M.E.T. (2001) Instability of the nuclear genome and the role of DNA repair. In Masoro, E.J. and Austad, S.N. (eds), *Handbook of the Biology of Aging*, 5th Edn. Academic Press, San Diego, CA, pp. 84–113.
- Vijg, J., Boerrigter, M.E.T.I. and Dollé, M.E.T. (1999) A transgenic mouse model for studying mutations *in vivo*. In Yu, B.P. (ed.), *Methods in Aging Research: Section D*. CRC Press, Boca Raton, FL, pp. 621–635.
- Dollé, M.E.T., Martus, H.-J., Novak, M., van Orsouw, N.J. and Vijg, J. (1999) Characterization of color mutants in *lacZ* plasmid-based transgenic mice, as detected by positive selection. *Mutagenesis*, **14**, 287–293.
- Dunson, D.B. and Tindall, K.R. (2000) Bayesian analysis of mutational spectra. *Genetics*, **156**, 1411–1418.
- Edwards, J.L. and Klein, R.E. (1961) Cell renewal in adult mouse tissues. *Am. J. Pathol.*, **38**, 437–453.
- Hinrichs, H.R., Petersen, R.O. and Baserga, R. (1964) Incorporation of thymidine into DNA of mouse organs. *Arch. Pathol.*, **78**, 245–253.
- MacPhee, D.G. (1995) Mismatch repair, somatic mutations and the origins of cancer. *Cancer Res.*, **55**, 5489–5492.
- Hendrich, B., Hardeland, U., Ng, H.-H., Jiricny, J. and Bird, A. (1999) The thymine glycosylase MBD4 can bind to the product of deamination at methylated CpG sites. *Nature*, **401**, 301–304.
- Sohal, R.S. and Weindruch, R. (1996) Oxidative stress, caloric restriction and aging. *Science*, **273**, 59–63.
- Lee, C.M., Weindruch, R. and Aiken, J.M. (1997) Age-associated alterations of the mitochondrial genome. *Free Radic. Biol. Med.*, **22**, 1259–1269.
- Reid, T.M., Feig, D.I. and Loeb, L.A. (1994) Mutagenesis by metal-induced oxygen radicals. *Environ. Health Perspect.*, **102** (suppl. 3), 57–61.
- Cariello, N.F., Douglas, G.R. and Soussi, T. (1996) Databases and software for the analysis of mutations in the human p53 gene, the human hprt gene and the *lacZ* gene in transgenic rodents. *Nucleic Acids Res.*, **24**, 119–120.
- Meng, Q., Singh, N., Heflich, R.H., Bauer, M.J. and Walker, V.E. (2000) Comparison of the mutations at Hprt exon 3 of T-lymphocytes from B6C3F1 mice and F344 rats exposed by inhalation to 1,3-butadiene or the racemic mixture of 1,2:3,4-diepoxybutane. *Mutat. Res.* **464**, 169–184.
- Loeb, L.A. (2001) A mutator phenotype in cancer. *Cancer Res.*, **61**, 3230–3239.
- Rogozin, I.B., Pavlov, Y.I., Bebenek, K., Matsuda, T. and Kunkel, T.A. (2001) Somatic mutation hotspots correlate with DNA polymerase error spectrum. *Nature Immunol.*, **2**, 530–536.
- Zeng, X., Winter, D.B., Kasmer, C., Kraemer, K.H., Lehmann, A.R. and Gearhart, P.J. (2001) DNA polymerase η is an A-T mutator in somatic hypermutation of immunoglobulin variable genes. *Nature Immunol.*, **2**, 537–541.
- Bult, C.J., Krupke, D.M., Naf, D., Sundberg, J.P. and Eppig, J.T. (2001) Web-based access to mouse models of human cancers: the Mouse Tumor Biology (MTB) Database. *Nucleic Acids Res.*, **29**, 95–97.
- Baross-Francis, A., Makhani, N., Liskay, R.M. and Jirik, F.R. (2001) Elevated mutant frequencies and increased C:G→T:A transitions in *Mlh1*^{-/-} versus *Pms2*^{-/-} murine small intestinal epithelial cells. *Oncogene*, **20**, 619–625.
- Prolla, T.A., Baker, S.M., Harris, A.C., Tsao, J.L., Yao, X., Bronner, C.E., Zheng, B., Gordon, M., Reneker, J., Arnheim, N., Shibata, D., Bradley, A. and Liskay, R.M. (1998) Tumour susceptibility and spontaneous mutation in mice deficient in *Mlh1*, *Pms1* and *Pms2* DNA mismatch repair. *Nature Genet.*, **18**, 276–279.
- Dollé, M.E.T., Snyder, W.K., van Orsouw, N.J. and Vijg, J. (1999) Background mutations and polymorphisms in *lacZ*-plasmid transgenic mice. *Environ. Mol. Mutagen.*, **34**, 112–120.